Characterization of MgB_2 Superconducting Hot Electron Bolometers

D. Cunnane, J. H. Kawamura, M. A. Wolak, N. Acharya, T. Tan, X. X. Xi, and B. S. Karasik

***Abstract*— Hot-Electron Bolometer (HEB) mixers have proven to be the best tool for high-resolution spectroscopy at the Terahertz frequencies. However, the current state of the art NbN mixers suffer from a small intermediate frequency (IF) bandwidth as well as a low operating temperature. MgB_2 is a promising material for HEB mixer technology in view of its high critical temperature and fast thermal relaxation allowing for a large IF bandwidth. In this work, we have fabricated and characterized thin-film (~ 15 nm) MgB_2-based spiral antenna-coupled HEB mixers on SiC substrate. We achieved the IF bandwidth greater than 8 GHz at 25 K and the device noise temperature < 4000 K at 9 K using a 600 GHz source. Using temperature dependencies of the radiation power dissipated in the device we have identified the optical loss in the integrated microantenna responsible as a cause of the limited sensitivity of the current mixer devices. From the analysis of the current-voltage (IV) characteristics, we have derived the effective thermal conductance of the mixer device and estimated the required local oscillator power in an optimized device to be ~ 1 μW.**

***Index Terms*—Hot Electron Bolometers, MgB_2, Superconducting Devices, Terahertz Mixers**

I. Introduction

SUPERCUNDUCTING HOT ELECTRON BOLOMETERS (HEBs) are the best choice for high-resolution spectroscopy in the far-infrared regime [1]. While there exist direct detectors with sensitivity far beyond the quantum noise limited mixers, heterodyne instruments allow for superior spectral resolution of $\lambda/\Delta\lambda \approx 10^6$-$10^7$ which is important for understanding chemical processes in star forming molecular clouds. SIS mixers have been shown to have sensitivity just a few times higher than the quantum limit, and have no bandwidth limitations due to small inherent time constants. They are, however, limited to frequencies below that set by the superconducting gap Δ, of the materials used. The cut-off frequency in practical SIS mixers does not exceed 1.3 THz [2], and beyond this, only HEBs have shown any promise. Hershel HIFI was a good example of HEBs exceeding the limitations of other detectors by scanning the galactic center (GC) for the CII line at 1.9 THz [3]. The state of the art HEB technology uses NbN films as thin as 3.5 nm [4]. While this technology is fairly mature, there are still some serious limitations which, if exceeded, could significantly benefit future FIR missions. The critical temperature, T_c, of NbN thin films ranges from about 9-11 K which limits operation to around 4.2 K. A combination of the electron-phonon time, $\tau_{e\text{-}ph}$, and the phonon escape time, τ_{es}, sets the fundamental limit for the intermediate frequency (IF) bandwidth. In the case of NbN, the IF bandwidth is generally of the order of 3 GHz [5] and while such a bandwidth is sufficient for spectroscopic studies of the GC at frequencies of 1.9 THz, Doppler broadening at this distance would mean that 7-8 GHz of bandwidth would be required for the same velocity span at the 4.7 THz OI line.

MgB_2 has a higher critical temperature than NbN which implies a stronger electron-phonon interaction and a much shorter time constant or larger IF bandwidth. The basic metallic structure has two superconducting gaps [6] which should not have a significant impact on the performance of an HEB made with MgB_2 films given the fact that HEB mixers operate in the resistive state when the gap is heavily suppressed. Indeed, some initial work has been done describing the potentially high performance of MgB_2 mixers [7-9]. The main issue in the past was the difficulty in developing ultrathin films with high critical temperature for HEB fabrication, necessary because the effective time constant which establishes the IF bandwidth is highly dependent on the film thickness d ($\tau_{es} \sim d$).

The hybrid physical-chemical vapor deposition (HPCVD) method of growing MgB_2 films has produced the highest quality films in the world [10]. The high pressure-high temperature process grows epitaxial films on SiC substrates with superconducting properties better than in the bulk material. It has been shown that these films can maintain good superconducting properties even at film thicknesses around 10 nm [11]. The island growth of HPCVD grown MgB_2 films, however, limits their thickness to around 7-8 nm [12].

In this work, we have developed a fabrication process for spiral antenna-coupled devices and done characterization of these devices for varying bath temperatures and pumping frequencies. We have shown that MgB_2 mixers have a behavior qualitatively similar to that in the state of the art NbN devices using DC measurements as well as with LO pumping

The research described in this paper was carried out at the Jet Propulsion Laboratory, California Institute of Technology, under a contract with the National Space and Aeronautics Administration. The work at Temple University was supported by the NASA Astrophysics Research and Analysis Program through a contract from JPL.

The research of D. Cunnane was supported by an appointment to the NASA Postdoctoral Program at the Jet Propulsion Laboratory, administered by Oak Ridge Associated Universities through a contract with NASA.

Authors D. Cunnane, J. H. Kawamura, and B. S. Karasik are with the Jet Propulsion Laboratory, California Institute of Technology, Pasadena, CA 91109 USA, e-mail: Daniel.P.Cunnane@jpl.nasa.gov.

Authors M. A. Wolak, N. Acharya, T. Tan, and X. X. Xi are with the Physics Department, Temple University, Philadelphia, PA 19122 USA.

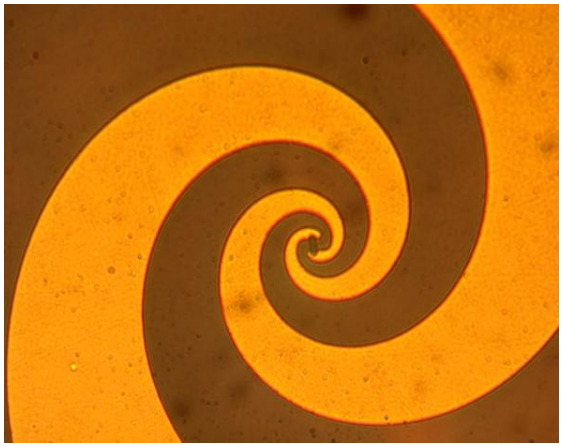

Fig. 1. Optical image of spiral antenna device #1 with bridge dimensions of 6 μm (L) × 4 μm (W) ×15 nm (T).

at 0.6, 1.6, and 2.5 THz. The IF bandwidth was measured as a function of temperature using monochromatic mixing at 600 GHz. The mixer gain bandwidth value in excess of 8 GHz has been obtained which is a remarkable advance in HEB mixer technology. In addition, the noise temperature was measured and the optical loss of the receiver setup was analyzed.

II. Experimental

A. Fabrication Process

The fabrication process began with the deposition of MgB_2 using the HPCVD process. The development of this film process is described elsewhere [11]. For this work, films ranged in thickness from 10-25 nm on 6H, semi-insulating SiC substrate. The substrate has been tested for THz transparency using Fourier transform spectroscopy and was found to be nearly lossless in the regions of interest for this work [13]. The films were then passivated using SiO_2.

After a bilayer film was obtained, UV lithography was used to define the HEB bridges and reactive etching in CHF_3 was used to remove the unprotected SiO_2. The deposition of the passivation layer was not done *in situ* with the MgB_2 deposition, so there was always some native oxide present, which impedes direct contact to the superconducting layer. To try to avoid this issue, ion milling was used to remove the oxide layer and a 150 nm-thick Au layer was deposited using e-beam evaporation. It has been shown before [14] that an *in situ* ion milling etch is required before a metal deposition to obtain good conductance through the interface. This process will be utilized in the next phase of our continuing development effort. The antenna was then defined using UV lithography. At this point, there was photoresist mask protecting both the antenna and the bridge as the resist from the bridge definition was left intact. Ion milling was then used to mill the unprotected areas all the way down to the substrate. At the end of this step, we were left with a bilayer structure for both the antenna and the bridge. The antenna consists of the thin MgB_2 layer and the thicker Au layer, while the bridge consists of the thin MgB_2 layer, still protected by the original SiO_2 passivation layer.

TABLE I
Mixer Device Characteristics

Device #	Film Thickness (nm)	Bridge Size (μm) Length x Width	T_c (K)	R_n (Ω)
1	20	6 × 4	38	4
2	15	4 × 4	33	50
3	20	4 × 4	38	5
4	10	3 × 2	35	42

The wafers were 1.5 cm × 1.5 cm, which yields nine 3 mm × 3 mm devices of spiral antenna-coupled, twin-slot antenna-coupled, and dc test chip configurations. All data presented in this work are from 4 different spiral antenna-coupled devices. Table 1 describes the parameters of the particular mixers reported in this work. Figure 1 shows an optical image of device #1.

B. Measurement Configuration

Measurements were carried out in an Infrared Laboratories cryostat with a Mylar optical window. As in a typical quasi-optical (QO) setup, samples were mounted on a Si lens and installed onto a mixer block. A cryogenic low noise amplifier (LNA) with the noise temperature $T_A \approx 5$ K as well as a room temperature amplifier were both used in the IF line. The 0.5-11 GHz bandwidth of amplification was limited by the LNA. A 5 mil Mylar sheet was used to thermally isolate the mixer block from the 4.2 K stage. This increases the minimum temperature to around 9-11 K but allows for heating of the sample up to T_c in the MgB_2 film without excessive boil-off of the liquid helium. The device was biased using a custom-designed bias circuit.

The devices were irradiated using either a 600 GHz solid state frequency multiplier source or an optically pumped FIR gas laser with strong lines around 1.6 and 2.5 THz. A schematic of the setup for noise temperature measurements is shown in Fig. 2 where a Mylar beam splitter is used to couple the high frequency source with the hot/cold loads. In the case of mixing measurements, to determine the IF bandwidth, two 600 GHz multipliers were used and the thermal radiation load was replaced with the additional multiplier source. The coupling of the radiation source to the mixer varies from about 2-20% of the incident power when loss due to the windows, beam splitter, and reflection from the lens are taken into account. The lower number also includes a 50% loss due to the polarization mismatch between the spiral antennas (circular polarization) and the solid-state sources (linear polarization) and poor coupling efficiency due to impedance mismatch of the device with the antenna. Typically, impedance matching is done by designing bridges to have normal resistance, R_n, of about 75 Ω. Currently, work is ongoing to tune the resistivity so that the smallest area device be well impedance matched to the antenna. This will minimize the device volume and hence the necessary LO power, which

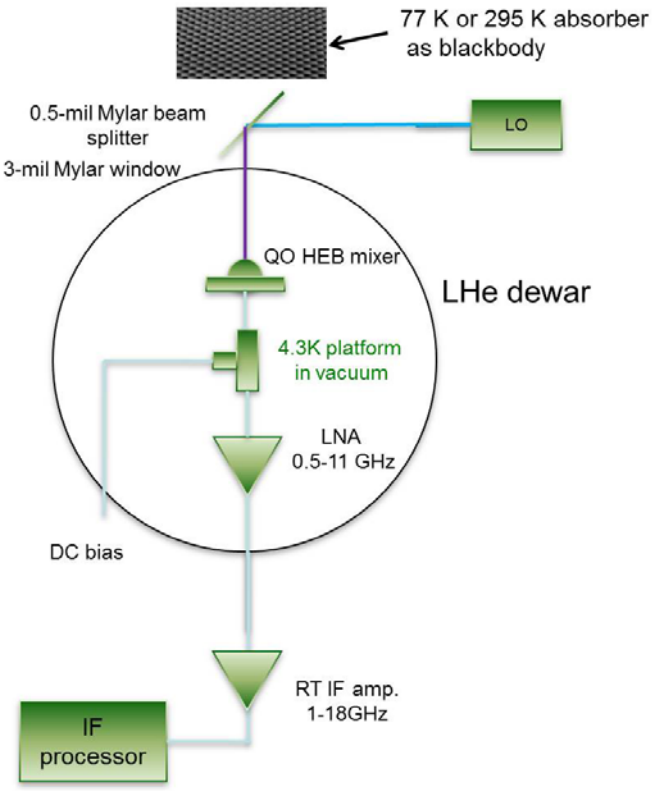

Fig. 2. Schematic diagram of noise temperature measurement setup.

may be somewhat higher than in NbN devices due to the larger change in electron temperature needed by pumping and larger effective thermal conductance at high temperature. While the large resistivity of NbN requires about 1/10 of a single square for proper impedance matching, MgB2 has much lower resistivity, so a few squares, or even a single square could have the desired impedance. When submicron MgB2 devices are fabricated, this will reduce the overall device volume by several times over NbN mixers. Since LO power is directly related to the HEB volume, this would correspond directly to a reduction in LO power required for optimal pumping. This is important, as LO technology is still limited above 1 THz with frequency multiplier based solid-state sources only reaching ~ 10 μW.

III. Results & Discussion

A. Superconducting Gap Frequency and RF Loss

Although the exact superconducting gap frequency, f_{Δ}, responsible for the radiation absorption may not be single valued, but rather a distribution due to the two gaps in MgB_2 [6], we were interested in finding some effective f_{Δ} to be used to approximate the gap for better understanding of the thin-film HEB devices. There were two ways we found to estimate

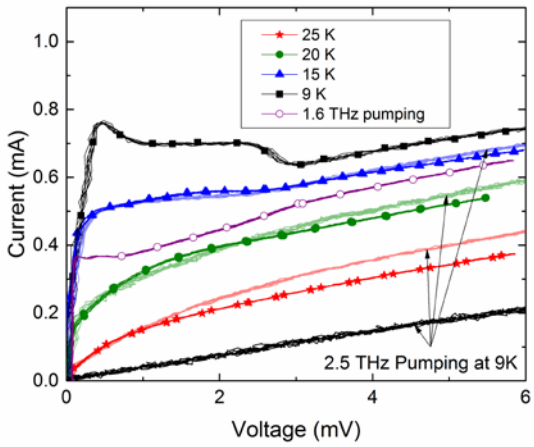

Fig. 3. IV curves of device #2 without LO pumping at different temperatures (closed symbols), 1.6 THz pumping at 9 K (open symbols), and 2.5 THz pumping at 9 K (no symbols).

the effective f_{Δ}. The first was to simply compare device characteristics when pumping with radiation of different frequencies. When above f_{Δ}, LO pumping should have a thermal effect on the IV characteristic, while below f_{Δ}, there should be mostly a heating of electrons in the current-driven resistive state. The latter effect would be a gradual increase of the resistance in the resistive state while maintaining a very sharp current switching to the resistive state. This effect was previously observed in NbN [15, 16]. The discrete spectral lines available using the gas laser did not allow for a very specific value, but rather a frequency range. The IV curves for several different temperatures and pumping levels of device #2 are shown in Fig. 3. It is evident that pumping the mixer at 2.5 THz is equivalent to heating because the IV curves compare very nicely to un-pumped IV curves at elevated bath temperatures. The pumping from a 1.6 THz source seems to occur in the "sub-gap mode" as the IV curve maintains sharp features, even when I_c is reduced to about half that of the low temperature I_c (purple plot with open circles in Fig. 3). This implies that the gap frequency around 10 K is somewhere between 1.6 and 2.5 THz.

The IF output power of device #3 is shown in Fig. 4. The curve with many sharp peaks (black squares) is from an un-pumped device and the smooth single peak (red circles) is from the same device pumped using a 2.5 THz LO. The sharp peaks of the un-pumped curve could be either of two anomalies. The first is that we are simply seeing many regions of the superconductor switch to the resistive state. Each peak represents a switch at that particular voltage. The other reason for the peaks could be some inter-grain weak links. In this case the peaks would represent a resonant frequency associated with a specific voltage by the AC Josephson effect. More investigation of this effect is necessary as weak links are undesirable in the HEB application. For the pumped state, it is evident from the sharp change of slope in IF power around 2 mV, that the pumping at 2.5 THz may not be a completely thermal effect for this device, which may be a result of a larger

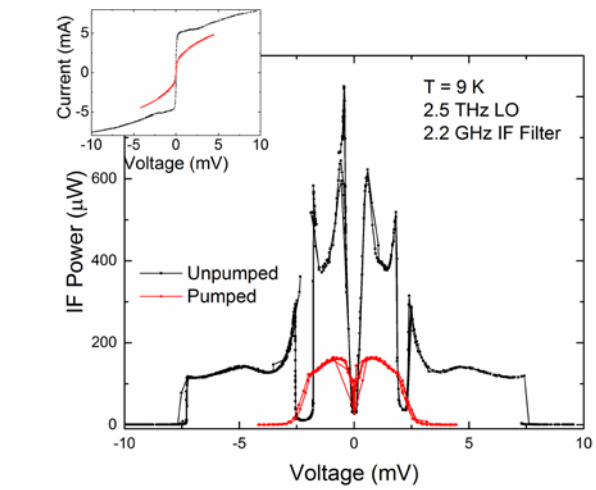

Fig. 4. IF power spectrum as a function of voltage bias for device #3 without LO (black squares) and pumped with 2.5 THz (red circles) at 9 K. There is a narrowband IF filter at 2.2 GHz. Inset shows the IV curves of the device both pumped and unpumped.

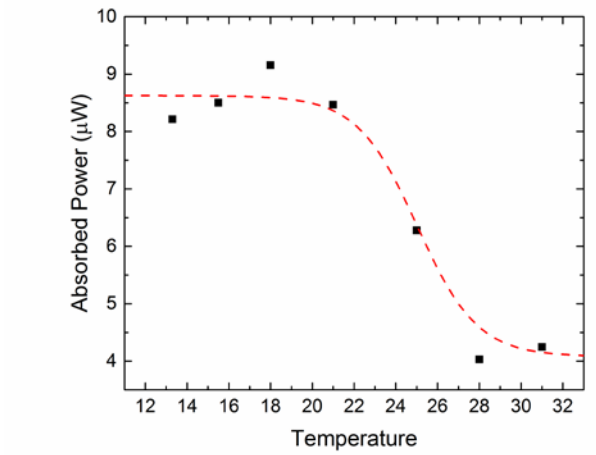

Fig. 5. Measured absorbed power in device #4 shown as a function of temperature. Power is taken to be the difference in P_{Joule} between a pumped and unpumped IV curve at the same temperature.

f_Δ due to the thicker film. The inset shows the respective IV curves from this device. This result also implies that there is good potential to use a thick MgB_2 antenna for a mixer designed for frequencies below f_Δ, where the superconductor has little to no RF loss.

The other method for determination of f_Δ takes advantage of the fact that we have poor contact between the MgB_2 and Au in the bilayer antenna structure. By measuring the absorbed radiation by the mixer and comparing it to the expected incident radiation at different temperatures, the temperature where the radiation frequency exceeds $f_\Delta(T)$ can be found. In this case, the frequency of the LO was 600 GHz. If the thin MgB_2 superconducting layer in the antenna contributes to any loss, there should be at least some temperature dependence associated with that loss.

The data presented in both Fig. 5 and Fig. 6 are taken by calculating the Joule power, P_{Joule}, of IV curves for device #4

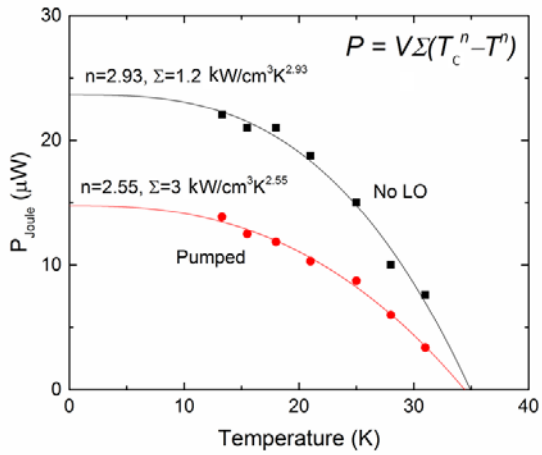

Fig. 6. P_{Joule} of device #4 measured along a constant resistance line fitted to the heat balance equation.

at different temperature intervals. Taking the dissipated Joule power along a constant resistance line (where the electron temperature is presumed constant) for both un-pumped and IV curves pumped by a constant LO can be used to estimate the absorbed power by the mixer. Choosing different constant resistance lines can vary the results by about a factor of 2, but we are only looking for some temperature dependent loss, and so the exact value is not needed. A constant resistance line which is half the device normal resistance was used.

Figure 5 shows the absorbed power measured in this way as a function of temperature. The dashed line is a guide for the eye. It is evident from the plot that there is a step at 25 K where absorbed power is reduced by a factor of two. It can be speculated that at this temperature, f_Δ is reduced below 600 GHz. While the measured absorbed power ranges from 4-8 μW, the expected incident power including all loss factors should be around 95 μW. The fact that we see some dominant temperature dependence in the loss implies that the radiation is confined to the thin superconducting layer. The order of magnitude or so of loss could easily be expected from such a thin superconducting layer, as the 10 nm film is much thinner than the penetration depth of MgB_2 [17]. Additional experiments which utilize a thick MgB2 layer under the antenna are currently being carried out to verify this while the contact issue is yet unaddressed. It may be possible to utilize a thick MgB_2 antenna even for frequencies above the gap frequency as the resistivity of MgB_2 is very low and may be comparable to a normal metal antenna.

B. Required LO power

Fig. 6 shows P_{Joule} for device #4 at different temperatures. The data fits well to the heat balance equation:

$$P = V\Sigma(T_C^{\,n} - T^n)$$

Where V is the device volume and Σ and n are material

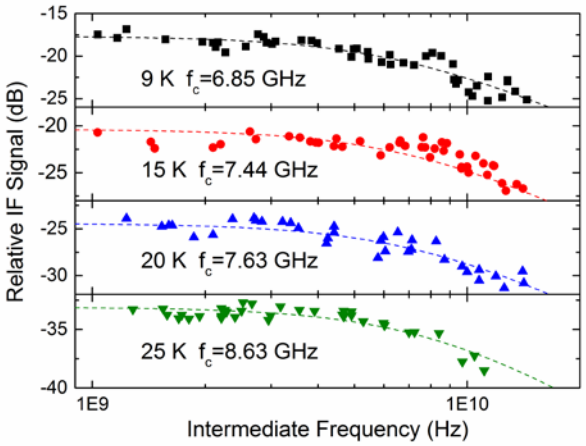

Fig. 7. Relative IF signal as a function of the IF frequency at temperatures of 9, 15, 20, and 25 K for device #2.

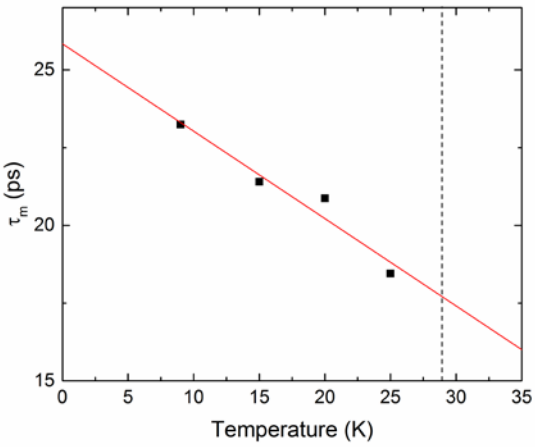

Fig. 8. The effective time constant for a MgB_2 HEB mixer as a function of temperature with a linear fitting. Dashed line indicates $0.8T_c$, above which the mixer may have reduced sensitivity.

constants. In this case, it fits well for $n = 2.93$. The value found for $\Sigma \sim 1$ kW/(cm^3 K$^{2.93}$) is noticeably lower than that derived for an apparently more robust 20 nm thick device in [13]. In any case, the data imply that necessary LO power (an electron temperature increase from 25 K to 36 K for an optimized mixer device (0.5 μm × 0.5 μm × 6 nm) may be about 1 μW or even less.

C. IF Bandwidth

A major figure of merit for HEB mixers is the IF bandwidth. Not only is Doppler broadening of the higher THz lines a major issue, but the tunability of LO sources at these high frequencies is significantly reduced. It has already been shown that MgB_2 HEBs have an increased IF bandwidth both for MBE grown films [9], as well as HPCVD grown films [13]. In this work, we looked at the bandwidth as a function of temperature. Figure 7 shows the IF output signal as a function of the intermediate frequency for measurements taken at different temperatures for device #2. The fittings are used to establish the cutoff frequency, which is given in each plot. One can see that mixing in the device is easily measured up to 25 K. It may even be possible to exceed this result, but the measurement set-up is not currently optimized to perform such experiments at higher temperatures. In the future, a cryocooler will be set up so that measurements can be taken all the way up to the T_c of the film. The question does remain as to whether the sensitivity of the device, once well established, will degrade with increased bath temperatures. For NbN devices, it has been shown that device sensitivity (noise temperature) remains nearly constant all the way to about $0.8T_c$ [18]. It is also well known that the bandwidth of these devices is related to the film thickness. The thickness effect is due to the acoustic phonon escape bottleneck in the net heat flow from the hot-electrons to the substrate. The characteristic phonon escape time τ_{es} is proportional to the films thickness. The device under study is made from 15 nm-thick film, so moving to devices made from 10 nm film could already achieve close to 10 GHz of bandwidth. We have found recently that films can be etched even thinner, down to 6 nm, without any loss in the superconducting properties, which will increase the bandwidth even further. Results from that experiment will be published elsewhere.

Fig. 8 shows a plot of the calculated mixer time constant, τ_m, as a function of temperature. The fit shows a linear dependence on temperature. The dashed line indicates $0.8T_c$ for this device. It would imply that a similar device with good sensitivity may operate at as high as 29 K with a bandwidth of 9 GHz. Note, this temperature dependence is not due to the $\tau_{e\text{-}ph}(T) \sim T^{-k}$ ($k \geq 1$) dependence (currently unknown) alone but rather an outcome of the combination of several processes (including electron-phonon interaction and acoustic phonon escape) as described by the Two-Temperature Model [19]. When more results become available a comprehensive numerical analysis may yield information on $\tau_{e\text{-}ph}$ and τ_{es}, similar to how it was done for NbN films [4, 20].

D. Noise Temperature

The mixer noise temperature was measured by comparing the IF output power for a 77 K radiation load with a room temperature load. Figure 9 shows the IF power as a function of bias voltage for device #2. This data was taken at 600 GHz. The system bath temperature was 9 K and the IF output is filtered at 2.2 GHz to ensure that the amplifiers are well within their dynamic range. The minimum noise temperature obtained from this curve at a bias voltage of 1.7 mV was 3900 K. This is several times greater than the current state of the art and is well explained by the amount of rf loss seen when measuring the incident power vs absorbed power (see Fig. 5). Hopefully, the noise temperature will be significantly improved as soon as the issue of poor contact between MgB_2 and Au is resolved or a device is integrated with a thick-film MgB_2 antenna.

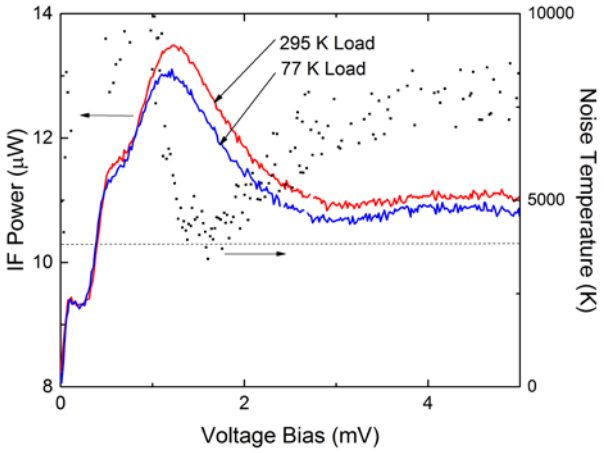

Fig. 9. IF output power (lines) and noise temperature (black squares) as a function of the mixer bias voltage.

IV. Conclusion

In summary, we have developed a process to fabricate MgB_2 HEBs utilizing HPCVD grown films. We have characterized these devices at dc as well as using 0.6 THz, 1.6 THz, and 2.5 THz radiation. The devices have a T_c around 36 K and have been shown to operate up to 25 K. We have found that the IF bandwidth of these devices far exceeds the state of the art NbN devices with a maximum bandwidth to date of 8.6 GHz. Although noise temperature of our MgB_2 devices is not yet to the level of NbN devices, it is within a reasonable limit considering the large optical loss in the current design. It is believed that when this issue is rectified the sensitivity of these devices will rival the state of the art. In the near future, we hope to show improved sensitivity of MgB_2 HEB mixer at 2.5 THz and at increased bath temperatures.

Acknowledgment

References

[1] J. Zmuidzinas and P. L. Richards, "Superconducting detectors and mixers for millimeter and submillimeter astrophysics," *Proc.IEEE*, vol. 92, pp. 1597-1616, Oct 2004.
[2] A. Karpov, D. Miller, F. Rice, J. A. Stern, B. Bumble, H. G. LeDuc, *et al.*, "Low noise 1 THz-1.4 THz mixers using Nb/Al-A1N/NbTiN SIS junctions," *IEEE Trans. Appl. Supercond.* vol. 17, pp. 343-346, Jun 2007.
[3] T. Velusamy, W. D. Langer, J. L. Pineda, P. F. Goldsmith, D. Li, and H. W. Yorke, "[CII] observations of H2 molecular layers in transition clouds," *Astron Astrophys*, vol. 521, L18, 2010.
[4] S. Cherednichenko, P. Yagoubov, K. Il'in, G. Gol'tsman, and E. Gershenzon, "Large Bandwidth of NbN Phonon-Cooled Hot-Electron Bolometer Mixers," in *27th EurMicrowave Conf.*, pp. 972-977, 1997.
[5] S. Cherednichenko, V. Drakinskiy, J. Baubert, J. M. Krieg, B. Voronov, G. Gol'tsman, *et al.*, "Gain bandwidth of NbN hot-electron bolometer terahertz mixers on 1.5 mu m Si3N4/SiO2 membranes," *J. Appl.Phys.*, vol. 101, no. 12, Jun 2007.
[6] H. J. Choi, D. Roundy, H. Sun, M. L. Cohen, and S. G. Louie, "The origin of the anomalous superconducting properties of MgB2," *Nat.*, vol. 418, pp. 758-760, Aug 2002.
[7] S. Bevilacqua, S. Cherednichenko, V. Drakinskiy, J. Stake, H. Shibata, and Y. Tokura, "Low noise MgB2 terahertz hot-electron bolometer mixers," *Appl. Phys. Lett.*, vol. 100, 033504, Jan 2012.
[8] S. Cherednichenko, V. Drakinskiy, K. Ueda, and M. Naito, "Terahertz mixing in MgB2 microbolometers," *Appl. Phys. Lett.*, vol. 90, 23507, Jan 2007.
[9] S. Bevilacqua, S. Cherednichenko, V. Drakinskiy, H. Shibata, Y. Tokura, and J. Stake, "Study of IF Bandwidth of MgB Phonon-Cooled Hot-Electron Bolometer Mixers," *Ieee Trans. THz Sci. Technol.*, vol. 3, pp. 409-415, Jul 2013.
[10] X. X. Xi, A. V. Pogrebnyakov, S. Y. Xu, K. Chen, Y. Cui, E. C. Maertz, *et al.*, "MgB2 thin films by hybrid physical-chemical vapor deposition," *Physica C*, vol. 456, pp. 22-37, Jun 2007.
[11] M. A. Wolak, N. Acharya, T. Tan, D. Cunnane, B. Karasik, X. X. Xi, "Fabrication and Characterization of Ultrathin MgB2 Films for Hot Electron Bolometer Applications," vol. 25, 2014 (Submitted).
[12] Y. Wang, C. Zhuang, X. Sun, X. Huang, Q. Fu, Z. Liao, *et al.*, "Ultrathin epitaxial MgB2 superconducting films with high critical current density and T-c above 33 K," *Supercond. Sci. & Technol.*, vol. 22, Dec 2009.
[13] D. Cunnane, J. Kawamura, B. S. Karasik, M. A. Wolak, and X. X. Xi, "Development of hot-electron THz bolometric mixers using MgB2 thin films,", *Proc. SPIE* pp. 91531Q-10, 2014.
[14] D. Cunnane, T. Tan, K. Chen, and X. X. Xi, "Study of Components for MgB2 RSFQ Digital Circuits," *IEEE Trans.Appl. Supercond.*, vol. 23, no. 3, Jun 2012.
[15] G. N. Goltsman, B. S. Karasik, O. V. Okunev, A. L. Dzardanov, E. M. Gershenzon, H. Ekstrom, *et al.*, "NBN HOT-ELECTRON SUPERCONDUCTING MIXERS FOR 100 GHZ OPERATION," *IEEE Trans. Appl. Supercond.*, vol. 5, pp. 3065-3068, Jun 1995.
[16] Y. Lobanov, E. Tong, R. Blundell, A. Hedden, B. Voronov, and G. Gol'tsman, "Large-Signal Frequency Response of an HEB Mixer: From 300 MHz to Terahertz," *IEEE Trans. Appl. Supercond.*, vol. 21, pp. 628-631, Jun 2011.
[17] B. B. Jin, T. Dahm, F. Kadlec, P. Kuzel, A. I. Gubin, E. M. Choi, *et al.*, "Microwave and terahertz surface resistance of MgB2 thin films," *J. Supercond.and Mag.*, vol. 19, pp. 617-623, Nov 2006.
[18] W. Zhang, N. Li, L. Jiang, Y. Ren, Q.-J. Yao, Z.-H. Lin, *et al.*, "Dependence of noise temperature of quasi-optical superconducting hot-electron bolometer mixers on bath temperature and optical-axis displacement," *Proc. SPIE* , pp. 684007-8, 2007.
[19] N. Perrin and C. Vanneste, "Response of superconductive films to a periodic optical radiation," *Phys. Rev. B*, vol. 28, pp. 5150-5159, 1983.
[20] A. D. Semenov, R. S. Nebosis, Y. P. Gousev, M. A. Heusinger, and K. F. Renk, "Analysis of the nonequilibrium photoresponse of superconducting films to pulsed radiation by use of a two-temperature model," *Phys. Rev. B*, vol. 52, pp. 581-590, Jul 1995.